

One pot synthesis, Structural, morphological, Optical Properties of Graphene Oxide/ NiO Nano composite suitable for super capacitor Applications.

M. Sappani Muthu¹, J. Agnes¹, P. Ajith¹, D. Prem Anand^{1*},

1. Materials Research Centre, Dept. of Physics, St. Xavier's College (Autonomous), Palayamkottai- 627002, Tamilnadu, India

Affiliated to Manonmaniam Sundaranar University, Abishekapatti 627012, Tirunelveli, Tamilnadu, India.

Reg: No: 19211282131025

Abstract:

In this paper, NiO nanoparticles Graphene sheet was prepared by an one pot synthesis method, which is one of the simplest technique. The as prepared NiO nanoparticles graphene sheets were characterized by XRD, FTIR, UV and SEM studies. XRD analysis confirms the crystallinity and phase purity of the sample. The functional groups in these prepared samples were confirmed by FTIR analysis. The UV visible spectra show the band gap at 3.25 eV. It was ascertained from SEM micrographs that the material has mesoporous morphology. This mesoporous morphology may be due to the increase of the surface to mass ratio of the material, which may increase the specific capacitance of the material.

Key Words; Nano Composite, Nickel Oxide, Graphene Oxide, Super capacitor application.

1. Introduction;

As a result of increase in energy consumption demands, conventional energy sources on the earth are getting extra used day by day. Thus the whole world has concentrated on energy related research. A renewable energy source is the best option for energy. The main problem with this type of energy is that it is not available all the time. As a result, it is necessary to store this type of energy when it is available so that it can be utilized whenever needed [1]. Li-ion batteries and super capacitors are widely used energy storage devices [2-4]. Conventional energy capacitors have high power density with low energy densities and the batteries have high energy density with low power density. A super capacitor with its high power and cycling is a device that is bridging the gap between the batteries and the convectional capacitors [5-6]. Metal oxides such as a SnO_2 , Fe_3O_4 , Fe_2O_3 , CO_3O_4 , RuO_2 , MoO_3 , ZnO , CuO , and WO_3 have been developed as a promising candidate for super capacitor electrodes [7-27]. NiO based nanostructures have been extensively applied as electrode material for lithium ion batteries, fuel cells, electronic films, gas sensors, and electrochemical super capacitors[30]. Because NiO is cheaper and easy to process using a variety of methods, therefore it deserves and continues to deserve, considerable research activities towards high performance electro chemical super capacitor applications. In this work graphene/ NiO Nano composites was prepared by one pot synthesis method. These prepared graphene/ NiO composites were characterized by XRD, FTIR, UV, and SEM studies.

Experimental;

2. Materials and Method

Graphite Flake powder (FG), sulfuric acid (H_2SO_4), potassium permanganate (KMnO_4), sodium nitrate (NaNO_3), hydrogen peroxide (H_2O_2), Hydrochloric acid (HCL), Ethanol, and Nickel Acetate $\text{C}_2\text{H}_6\text{NiO}_4 \cdot 4\text{H}_2\text{O}$

2.1 Synthesis of graphene Oxide (GO)

Graphite oxide (GO) was prepared by a modified Hummers method, and the preparation is described in a typical process. Concentrated H_2SO_4 (70ml) was added in the mixture of graphite (FG) powder (1.5g), sodium nitrate (3.0g) NaNO_3 in the flask and then cooled on a ice bath and stirred for 45 minutes. KMnO_4 (9.0g) of potassium permanganate was added very slowly and temperature was controlled under 293 k. After stirring for 2 h. in the ice bath, the mixture was transferred into the water bath and kept at 308 k for 1h. The water (140 ml) was followed to add into the mixture and caused its temperature slowly up to 371 k maintain at the temperature for 1h. The reaction temperature was found to increase rapidly to 373k with effervescence and the color changed to brown. Then the mixture 30ml of H_2O_2 was added to the above solution and the color changed to yellow. Finally the solid mixture was separated by the filtration and high speed centrifugation (6000rpms) washed with Hcl solution and water respectively and dried in vacuum at 323k for 96 h to get GO.

GO(50mg) was dispersed in ethanol (65ml) by sonication for 3h and then the Nickel Acetate $C_2H_6NiO_4 \cdot 4H_2O$ powder was added into the solution according to NiO/GO mass percent 50:50 ratio respectively and continued to ultrasonic dispersal for 1h. The obtained suspension was sealed in to a Teflon-lined autoclave (100ml) and heated at 473 k for 12 h. The last products were filtered washed with ethanol and dried in vacuum at 323 k for 24h. For comparison pure NiO and graphene sheets (GS) were produced by the above method.

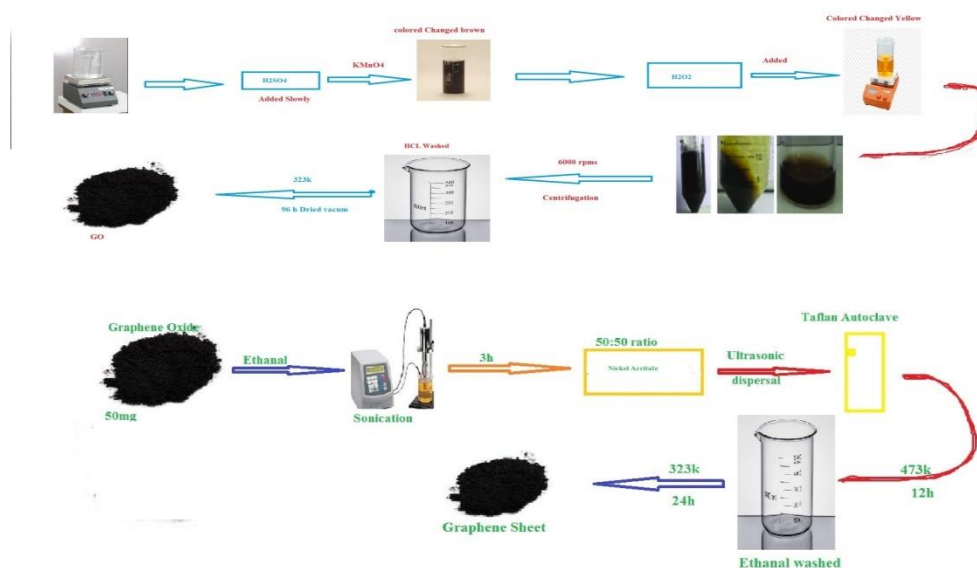


Figure 2.1 Synthesis of Graphene Oxide/ NiO

3. Characterization

The crystallographic structure of Graphene/ NiO Nano composites were determined by X-ray diffraction system PAN analytical Expert instrument equipped with CuKa ($\lambda=1.5406\text{\AA}$) radiation FTIR analysis were done on the instrument Perkin Elmer Spectrometer operating at $4000-400\text{cm}^{-1}$. The morphological and elemental analysis was done on Philips XL30 electron microscope.

4. Result and discussion

4.1 XRD analysis

X-ray powder diffraction is to most common analysis for the generalized characterization of crystalline and nano material which range of atom and also to verify the oxidation of single crystal or nano crystal. X-ray diffraction analysis of nano Graphene Oxide sample. is shown in the Figure 4.1a. The average crystalline size 'D' of the as obtained Graphene oxide nanoparticles were estimated by Debye-Scherrer equation

$$D=0.89 \lambda/\beta \cos \theta$$

Where λ is the wavelength of the incident beam ($\lambda =1.5406\text{\AA}$) and β is the full width at half maximum and θ is the Bragg's diffraction angle. It was discovered that the average particle size was 21nm. In order to corroborate the peak structure, one can compare them to standard

available data, 15.15°, 19.59°, 21.83°, 24.83°, 27.06°, 32.92°, 43.75°, 45.55°, 55.89°, XRD pattern we can see a prominent peak at 27.06° corresponding a prominent Plane. And also there is a clear shift in 2θ value and full width maxima for a prominent Plane this can be observed as we go from peak 21.51°, and also sharp peak at intense peak at 27.06°, the all this peak which conform the good space structure the interlayer facing of nano graphite oxide. According to the peak at $2\theta = 70^\circ$ this value is higher the interlayer facing of graphite powder this is due to the presence of oxygenated functional group and interrelated water molecules from the spectrum there is diffraction $2\theta = 27.06^\circ$ (MS Amir Faiz, et al 2020) which is mainly due to oxidated graphite the diffraction peak of nano graphene oxide is found to around 27.06° around which crosspound to the highly organized structure with on interlayer structure. (Zaaba, N.I., et al 2017), (Paulchamy. B. et al. 2015), (venkateswara Rao. K., et al. 2013) The disappearance peak at 55.89° appearance of peak at 45.56° shows that product is computes oxidation after the chemical oxidation and exfoliation indicating the presence of de spacing of nano graphene oxide crystalline lattice. The XRD patterns agree well with the tetragonal hausmannite of the Graphene Oxide and it is confirmed that Graphene Oxide nanoparticles are of tetragonal hausmannite crystalline structure. [1,2] the second layer of Figure 4.1 b. shows the XRD spectrum of Nickel oxide/graphene sheets. The diffraction peaks at 37.6°, 43.7°, and 63.9°, are the typical character diffraction peaks of NiO which are in accordance with the JCPDS data for NiO (card no; 47-1049) and the peaks around at $2\theta = 37.7^\circ$, 43.7°, and 63.7° were identified as [111], [200], and [220] respectively. From the XRD spectrum there is no distinctive peak of graphene oxide ($2\theta = 10.9^\circ$) or graphite flakes ($2\theta = 21.6^\circ$) confirming that graphene oxide was well condensed [37]. Both the graphene and the composite showed the typical 2θ peak for graphene at about 26°, corresponding to the d-spacing of about 0.36nm. Although the d-spacing is higher than that of natural graphite (0.33nm) the value are similar to pure graphene and the composites, suggesting that NiO nano crystalline have not greatly affected the origin of the graphene layer [38].

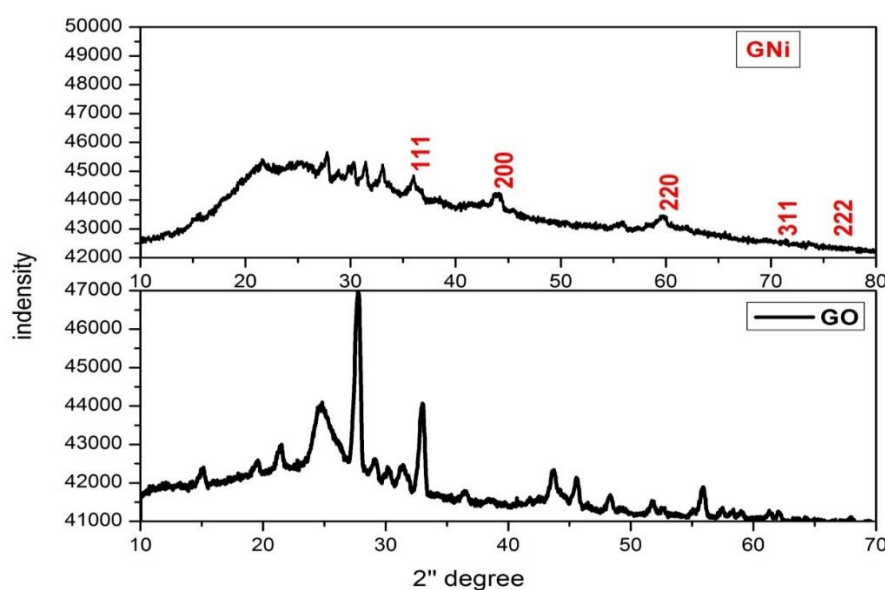


Figure 4.1 XRD Pattern of Nano Graphene Oxide and NiO nanocomposite .

4.2 FTIR Spectral Analysis

Essentially it's a method used to Infrared spectra of an infrared-absorbing solid, a liquid, or a gas to determine their absorption, emission, and photoconductivity are obtained, and can also be An unknown mixture can be quantitatively analyzed using this technique. It is expected that after the oxidation processes, the iterative of the peaks is proportional to the amount of material present. The produced GO exhibits a peak of 619 cm^{-1} , which is ascribed to the C-O bond, showing the existence of oxide confirming the oxidation process produces functional groups, as shown in Figure 4.2a. The peaks in the range from 1571 cm^{-1} to 1111 cm^{-1} show that the C = C bond, which remains An oxidized and oxidized sample processes, the water Broad peaks indicate the amount of water absorbed by GO 2925 cm^{-1} to 3416 cm^{-1} , This is produced by the OH- Being a high-quality game is one of the main advantages of GO absorbent substance, as seen by its propensity to create a Syrup that appears jelly-like, contributes to the trace of H_2O molecules. (MS Amir Faiz, et al 2020, paulchamy et al 2015) The FTIR spectrum of NiO/graphene nanocompoite is shown in the Figure 4.2 b. The spectrum Showed vibrational bands at about 3432 cm^{-1} , 1612 cm^{-1} , 1114 cm^{-1} , and 618 cm^{-1} which is typical for α - type hydroxide [39-40]. Although the broadness of the peaks for the composites is not as the same for Nickel hydroxide, the characteristics peaks are common to both the samples. Vibrational bands for free hydroxyl groups at 3432 cm^{-1} and for H-banded to water at 3405 cm^{-1} seen to be well separated and small in the composite compared to the broad band of pure NiO intermediate sample although there is no apparent shift in the band position. This result suggests that the free off vibration is low in the composite. The FTIR spectrum displays a broad peak at 111 cm^{-1} corresponds to the metal oxide (M-O) stretching vibration mode and confirms successfully the synthesis of NiO nanoparticles. The extra peaks obtained at 1317 and 1627 cm^{-1} are due to the rocking and wagging vibration transition of the O-H group and the small peak at 3432 cm^{-1} is for O-H stretching vibration mode of the physically adsorbed water the synthesized NiO/Graphene sheet shown peaks at $1052, 1615$ and 1737 cm^{-1} for C-O, C=C and C=O stretching vibration mode .

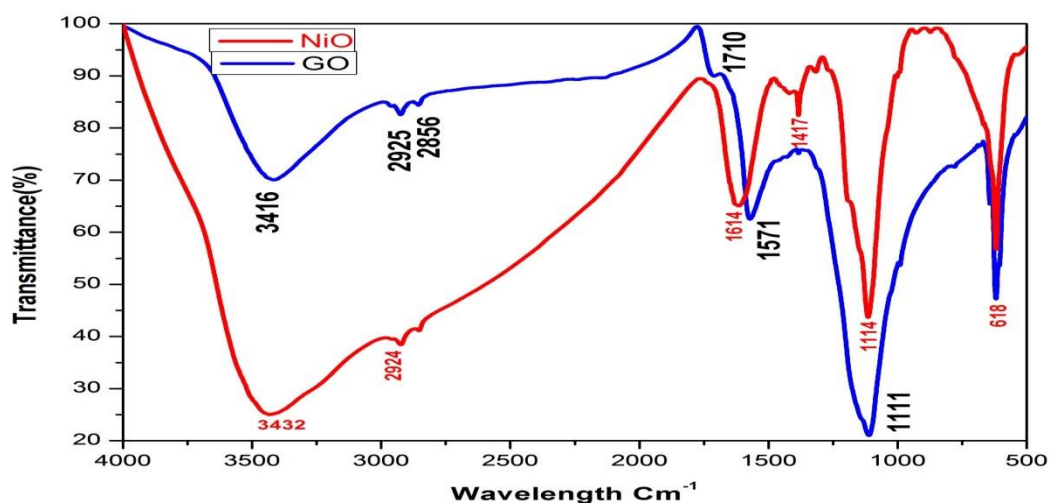


Figure 4.2 FTIR analysis of Nano Graphene oxide and NiO nanocompoite.

4.3 UV-Vis NIR analysis

UV- Visible spectra of Nickel oxide/graphene sheet is shown in the Figure 4.3.b, there are two characterization absorption bands in the UV- Visible spectra. The absorption band centered at 271 nm is attributed to $\pi \rightarrow \pi^*$ transitions of aromatic C-C bands. The shoulder centered at 298 nm corresponds to $n \rightarrow \pi^*$ transitions of C=O bonds. We can see from the spectra that the absorption increases fairly and attains a constant value. It is also found that the absorption peak at 323 nm red shifts to 271 nm and the other absorption band at 296 nm is completely removed. The UV- Visible spectra results reveal that the Oxygen containing functional groups on the surface of graphene are mostly removed and the electronic conjugation within graphene Nano sheets is restored solvothermal synthesis. Similar results were also obtained by *yu et al*[41] and *Xu et al*[42]. In the next step, the energy band gap of the NiO, graphene sheets nanocomposite was calculated by Tauc relation[43],

$$\alpha (\alpha h\nu) n = A (h\nu - E_g) \quad \text{Where } \alpha, A, h, \nu, n (=1/2)$$

for direct band gap and E_g are the optical absorption coefficient absorbance, planks constant, frequency of light, constant, related to mode of transition and band gap energy respectively band gap energy was calculated by extrapolating the straight region of the graph plotted between $h\nu$ and $(\alpha h\nu)^2$ the results show that the band gap energy was found to be 3.25eV as shown in the Fig. 4.3 a.

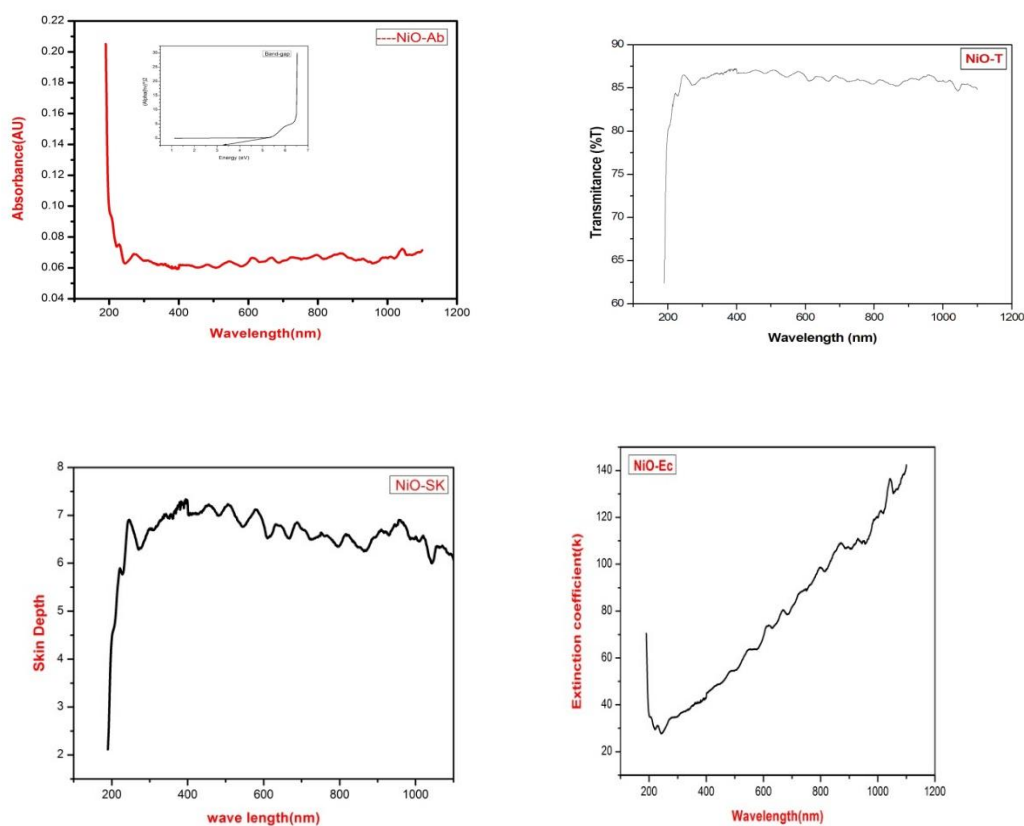


Figure 4.3 a) Absorption and Tauc's plot, b) Transmittance, c) Skin Depth, d) Extinction Coefficient.

Skin Depth

The optical penetration depth of a substance is the depth to which light or other electromagnetic radiation may enter it. Skin depth $\delta = 1/\alpha$, α – Absorption coefficient, as shown in Figure 4.3. c) It can be seen that skin depth increases up to 246 nm and then decreases. The minimum value of skin depth was approximately 308 nm and then began to climb until it reached its maximum at 387 nm. This demonstrates that electromagnetic radiation with a wavelength of around 398 nm is reaching the substance more deeply.

Extinction Coefficient

The degree to which a chemical species or material absorbs light at a specific wavelength. It is determined by the produced material's structure and chemical makeup. The extinction coefficient is a measure of electromagnetic radiation absorption in a material and loss owing to scattering. $K = \alpha\lambda/4M$, α – Absorption Coefficient, λ is the Wavelength, from Figure 4.4 d) Extinction coefficient shortly decreases and increases as wavelength increase after 244nm it is increased after 890 nm it goes linear or says become constant

4.4 SEM analysis;

Morphological examinations were executed by SEM micrographs of Nickel Oxide/graphene Nano Sheets are shown in the Figures.4.4. The micrograph in Fig4.4.a has a porous flake like structure with the graphene sheet well connected with each other. This is an indication that the graphene has been in foliated during the preparation process this may be due to the distorted graphene sheets when Oxygen and other functionality groups are attached to the sheets of graphene to form Nickel Oxide/graphene Nano composites. The micrographs are evenly distributed and well-connected with graphene. Indicating that graphene sheets in NiO overlapped each other. From the Fig 4.4.b micrograph, it is clear that show the sheets are stalked together. From the Fig 4.4.c, micrograph of the SEM images, it is clearly seen that the particles are in spherical in shape. The surface is not smoothing, but the particle size lies well within the Nano range. Hence it confirms that the particle is in the Nano scale.

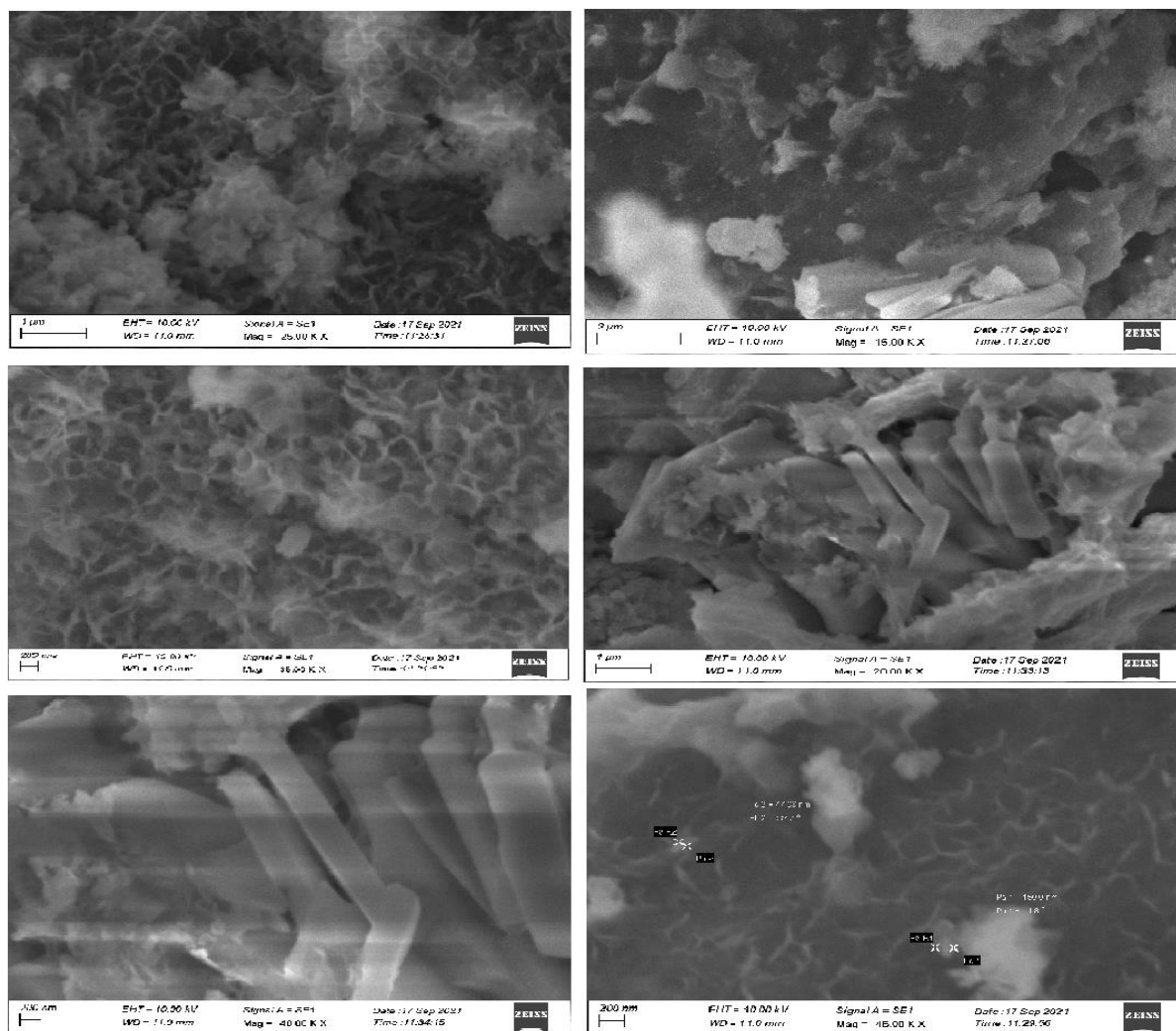


Figure 4.4 SEM analysis of GO and GO composite NiO with a mass percent of 50:50

For suitable super capacitor Application

Nanocomposite-based devices for electrical and optoelectronic applications, such as light emitting diodes, photodiodes, solar cells, gas sensors, and field effect transistors, as well as composite electrolyte materials for applications such as solid-state lithium batteries. A supercapacitor is located between the capacitor and the battery. Also known as a supercapacitor, a double layer capacitor, or an ultracapacitor. When compared to a standard capacitor, a supercapacitor has an extremely large capacitance and a low voltage rating. A supercapacitor stores energy in a double layer of charge between the ions of the electrode. Cordless electric screwdriver that charges in a matter of minutes. LED flashlights are used in digital cameras. Supercapacitors are utilised in ICs for power supply stabilisation in laptops and portable devices, where it substitutes electrolytic capacitor banks.

5. Conclusion

A NiO Graphene Sheets nano composite were successfully synthesized by solvothermal process. The results obtained from XRD, FTIR, SEM, UV showed that NiO nanoparticles were deposited on graphene, XRD confirmed the pure degree of the crystalline of the sample. The average nano composite size was found to be 13nm. The functional groups were confirmed by FTIR spectra. SEM images show the uniform distribution on NiO nanoparticles a graphene structure.

Acknowledgements

The authors would like to thank the research which was supported and guided by Dr. Akhila Kumar sagu. CSIR principal scientist and Dr. Mageshkumar SPO, CSIR Chennai Tharamani complex Chennai, for their constant support and encouragement. The authors are very grateful for the constant support provided by Rev. Dr. S. Mariadoss S.J, the principal of St. Xavier's College, Palayamkottai, and Rev. Dr. Alphonse Manickam S.J, the secretary of St. Xavier's College, Palayamkottai

Reference:

1. Varshney, B., Siddiqui, M. J., Anwer, A. H., Khan, M. Z., Ahmed, F., Aljaafari, A., ... & Azam, A. (2020). Synthesis of mesoporous SnO₂/NiO nanocomposite using modified sol-gel method and its electrochemical performance as electrode material for supercapacitors. *Scientific reports*, 10(1), 1-13.
2. Singh, A., & Chandra, A. (2013). Graphene and graphite oxide based composites for application in energy systems. *physica status solidi (b)*, 250(8), 1483-1487.
3. Luo, X., Wang, J., Dooner, M., & Clarke, J. (2015). Overview of current development in electrical energy storage technologies and the application potential in power system operation. *Applied energy*, 137, 511-536.
4. Arico, A. S., Bruce, P., Scrosati, B., Tarascon, J. M., & Van Schalkwijk, W. (2011). Nanostructured materials for advanced energy conversion and storage devices. *Materials for sustainable energy: a collection of peer-reviewed research and review articles from Nature Publishing Group*, 148-159.
5. Chandra, A., Roberts, A. J., Yee, E. L. H., & Slade, R. C. (2009). Nanostructured oxides for energy storage applications in batteries and supercapacitors. *Pure and Applied Chemistry*, 81(8), 1489-1498.
6. Yu, Z., Tetard, L., Zhai, L., & Thomas, J. (2015). Supercapacitor electrode materials: nanostructures from 0 to 3 dimensions. *Energy & Environmental Science*, 8(3), 702-730.
7. Manikandan K, Dhanus Kodi S, Maheswari N, Muralidharao G. AIP. Confe. Proc.1731,50048 (2016)
8. Xu, S., You, L., Zhang, P., Zhang, Y., Guo, J., & Wang, C. (2013). Fe₃O₄@ coordination polymer microspheres with self-supported polyoxometalates in shells exhibiting high-performance supercapacitive energy storage. *Chemical Communications*, 49(24), 2427-2429.

9. Liu, M., Zhou, L., Luo, X., Wan, C., & Xu, L. (2020). Recent advances in noble metal catalysts for hydrogen production from ammonia borane. *Catalysts*, *10*(7), 788.
10. Sun, H., Chen, B., Jiao, X., Jiang, Z., Qin, Z., & Chen, D. (2012). Solvothermal synthesis of tunable electroactive magnetite nanorods by controlling the side reaction. *The Journal of Physical Chemistry C*, *116*(9), 5476-5481.
11. Xia, H., Hong, C., Li, B., Zhao, B., Lin, Z., Zheng, M., ... & Aldoshin, S. M. (2015). Facile synthesis of hematite quantum-dot/functionalized graphene-sheet composites as advanced anode materials for asymmetric supercapacitors. *Advanced Functional Materials*, *25*(4), 627-635.
12. Lee, K. K., Chin, W. S., & Sow, C. H. (2014). Cobalt-based compounds and composites as electrode materials for high-performance electrochemical capacitors. *Journal of Materials Chemistry A*, *2*(41), 17212-17248.
13. Varshney, B., Siddiqui, M. J., Anwer, A. H., Khan, M. Z., Ahmed, F., Aljaafari, A., ... & Azam, A. (2020). Synthesis of mesoporous SnO₂/NiO nanocomposite using modified sol-gel method and its electrochemical performance as electrode material for supercapacitors. *Scientific reports*, *10*(1), 1-13.
14. Park, J. H., Ko, J. M., & Park, O. O. (2003). Carbon nanotube/RuO₂ nanocomposite electrodes for supercapacitors. *Journal of the Electrochemical Society*, *150*(7), A864.
15. Gujar, T. P., Shinde, V. R., Lokhande, C. D., Kim, W. Y., Jung, K. D., & Joo, O. S. (2007). Spray deposited amorphous RuO₂ for an effective use in electrochemical supercapacitor. *Electrochemistry communications*, *9*(3), 504-510.
16. Chang, K. H., & Hu, C. C. (2004). Hydrothermal synthesis of hydrous crystalline RuO₂ nanoparticles for supercapacitors. *Electrochemical and Solid State Letters*, *7*(12), A466.
17. Xue, J., Wu, T., Dai, Y., & Xia, Y. (2019). Electrospinning and electrospun nanofibers: Methods, materials, and applications. *Chemical reviews*, *119*(8), 5298-5415.
18. Lu, T., Pan, L., Li, H., Zhu, G., Lv, T., Liu, X., ... & Chua, D. H. (2011). Microwave-assisted synthesis of graphene-ZnO nanocomposite for electrochemical supercapacitors. *Journal of Alloys and Compounds*, *509*(18), 5488-5492.
19. Zhao, B., Xu, J., Liu, Y., Fan, J., & Yu, H. (2021). Amino group-rich porous g-C₃N₄ nanosheet photocatalyst: Facile oxalic acid-induced synthesis and improved H₂-evolution activity. *Ceramics International*, *47*(13), 18295-18303.
20. Xue, C., Lv, Y., Zhang, F., Wu, L., & Zhao, D. (2012). Copper oxide activation of soft-templated mesoporous carbons and their electrochemical properties for capacitors. *Journal of Materials Chemistry*, *22*(4), 1547-1555.
21. Varshney, B., Siddiqui, M. J., Anwer, A. H., Khan, M. Z., Ahmed, F., Aljaafari, A., ... & Azam, A. (2020). Synthesis of mesoporous SnO₂/NiO nanocomposite using modified sol-gel method and its electrochemical performance as electrode material for supercapacitors. *Scientific reports*, *10*(1), 1-13.
22. Miskei, M., Gregus, A., Sharma, R., Duro, N., Zsolyomi, F., & Fuxreiter, M. (2017). Fuzziness enables context dependence of protein interactions. *FEBS letters*, *591*(17), 2682-2695.

23. Lang, J. W., Kong, L. B., Wu, W. J., Luo, Y. C., & Kang, L. (2008). Facile approach to prepare loose-packed NiO nano-flakes materials for supercapacitors. *Chemical Communications*, (35), 4213-4215.
24. Liang, K., Tang, X., & Hu, W. (2012). High-performance three-dimensional nanoporous NiO film as a supercapacitor electrode. *Journal of Materials Chemistry*, 22(22), 11062-11067.
25. Poizot, P. L. S. G., Laruelle, S., Grugeon, S., Dupont, L., & Tarascon, J. M. (2000). Nano-sized transition-metal oxides as negative-electrode materials for lithium-ion batteries. *Nature*, 407(6803), 496-499.
26. MacLachlan, M. J., Coombs, N., Bedard, R. L., White, S., Thompson, L. K., & Ozin, G. A. (1999). Mesostructured metal germanium sulfides. *Journal of the American Chemical Society*, 121(51), 12005-12017.
27. Wang, X., Song, J., Gao, L., Jin, J., Zheng, H., & Zhang, Z. (2004). Optical and electrochemical properties of nanosized NiO via thermal decomposition of nickel oxalate nanofibres. *Nanotechnology*, 16(1), 37.
28. Vehmeijer, F. O., Küpers, L. K., Sharp, G. C., Salas, L. A., Lent, S., Jima, D. D., ... & Felix, J. F. (2020). DNA methylation and body mass index from birth to adolescence: meta-analyses of epigenome-wide association studies. *Genome medicine*, 12(1), 1-15.
29. Fantini, M. C. A., Ferreira, F. F., & Gorenstein, A. (2002). Theoretical and experimental results on Au–NiO and Au–CoO electrochromic composite films. *Solid State Ionics*, 152, 867-872.
30. Mozetič, M., Vesel, A., Primc, G., Eisenmenger-Sittner, C., Bauer, J., Eder, A., ... & Montelius, L. (2018). Recent developments in surface science and engineering, thin films, nanoscience, biomaterials, plasma science, and vacuum technology. *Thin Solid Films*, 660, 120-160.
31. Miller, E. L., & Rocheleau, R. E. (1997). Electrochemical behavior of reactively sputtered iron-doped nickel oxide. *Journal of the Electrochemical Society*, 144(9), 3072.
32. Narasimharo k, venkata ramana G, Sreedhar D, and Vasudevarao V, J.Mat Sci.Eng 2016.5;6
33. Iresha R.M.Kottegoda, Nurul Hayati idvis, Linlu,Jia-zbao wang, Hua-Kun liu, Electrochemical Acta 56 (2011) 5815-5822
34. Wen, J., Li, S., Li, B., Song, Z., Wang, H., Xiong, R., & Fang, G. (2015). Synthesis of three dimensional Co₉S₈ nanorod@ Ni (OH)₂ nanosheet core-shell structure for high performance supercapacitor application. *Journal of Power Sources*, 284, 279-286.
35. Bora, M. (2013). Homogeneous precipitation of nickel hydroxide powders. *Retrospective Theses and Dissertations. Iowa State University*, 199, 199.
36. Yin, Y., Yu, S., Yang, X., Liu, J., & Jiang, G. (2015). Source and pathway of silver nanoparticles to the environment. In *Silver nanoparticles in the environment* (pp. 43-72). Springer, Berlin, Heidelberg.
37. Xu, Z., Gao, H., & Guoxin, H. (2011). Solution-based synthesis and characterization of a silver nanoparticle–graphene hybrid film. *Carbon*, 49(14), 4731-4738.
38. Tauc, J. (1968). Optical properties and electronic structure of amorphous Ge and Si. *Materials Research Bulletin*, 3(1), 37-46.